Acta Scientiarum
http://periodicos.uem.br/ojs
ISSN on-line: 1807-8664
Doi: 10.4025/actascitechnol.v45i1.61562

Optimization of reinforced concrete columns via genetic algorithm

Isabella Silva Menezes[1*], Vinicius Navarro Varela Tinoco[1], André Luis Christoforo[1], Florisvaldo Cardozo Bomfim Junior[2] and Tarniê Vilela Nunes Narques[2]

[1]Programa de Pós-graduação em Engenharia Civil, Universidade Federal de São Carlos, Rodovia Washington Luís, km 235, s/n., 13565-905, São Carlos, São Paulo, Brasil. [2]Universidade de Uberaba, Uberaba, Minas Gerais, Brasil. *Author for correspondence: E-mail: ec.isabellasm@gmail.com

ABSTRACT. Reinforced concrete is an essential material in the modern world, and the use of genetic algorithms that aim at the optimization of the structures of this material is an increasingly widespread tool. The objective of the present work was to propose a method by means of a Genetic Algorithm to find the optimized geometry of a rectangular reinforced concrete column based on its cost. The two main parts of the work were developed as: a geometry verification algorithm that received height, base, layers in x and y directions, diameters of transverse and longitudinal steel rebar as the main parameters of the proposed sections, and a genetic algorithm that generated 240 random populations and selected them, crossed among them and then generated new 100 generations of individuals, followed by selection of optimized ones by its penalized cost. The generations had more and more favorable individuals and it was possible to determine an optimized geometry for the proposed example. It is, therefore, concluded that genetic algorithms are useful tools for optimizing reinforced concrete parts with multiple parameters. The proposed algorithm methodology really checks and selects the best individuals for the sections proposed by engineers, and larger initial populations are essential to find a minimum global cost among the different options.

Keywords: concrete structures; Scilab; programming; geometry optimization.

Received on November 16, 2021.
Accepted on March 3, 2022.

Introduction

In the form of the most used industrial product in the world, reinforced concrete has several design techniques based on the theories of materials' behavior, and also on the normalizations provided by the countries' technical associations. In Brazil, the Brazilian Association of Technical Standards determines, by the NBR 6118 (Associação Brasileira de Normas Técnicas [ABNT], 2014), that columns are "[...] straight axis linear elements, usually arranged vertically, in which normal compression forces are preponderant". Its design, therefore, must be given mainly in the function of the normal compression characteristic, so that the main other consideration is the eccentricity to which it is applied and generated by constructive considerations of instability, absorption of bending moment coming from the beams, considerations of second-order effects or creep. Figure 1 presents the domains for the design of reinforced concrete parts in the ultimate limit state, as they should be considered for designers, which represent the elongation (left) and shortening (right) of the reinforced concrete cross-section.

A large part of the problematic about the design of reinforced concrete columns with rectangular cross-sections is due to the fact that, commonly, the analysis of the domains must be carried out in different directions. The main practical design model for columns is presented by Carvalho and Pinheiro (2013) and uses approximate equations to define the required cross-section and abacuses for specific dispositions of the steel bars in the concrete cross-section that receive dimensionless forces as parameters. This form of design, as it gives the professional engineer the freedom to direct the design to a desired geometry, removes the possibility of developing techniques of optimization of the referred parts. Araújo (2014), despite not presenting a less empirical model for the determination of the reinforced concrete cross-section, presents the pure and analytical design high complexity differential equations are used to obtain the required steel bar section in terms of its area. The need for column optimization is an ever-present concern in engineering, given that the designer's role is to ensure safety with limited resources.

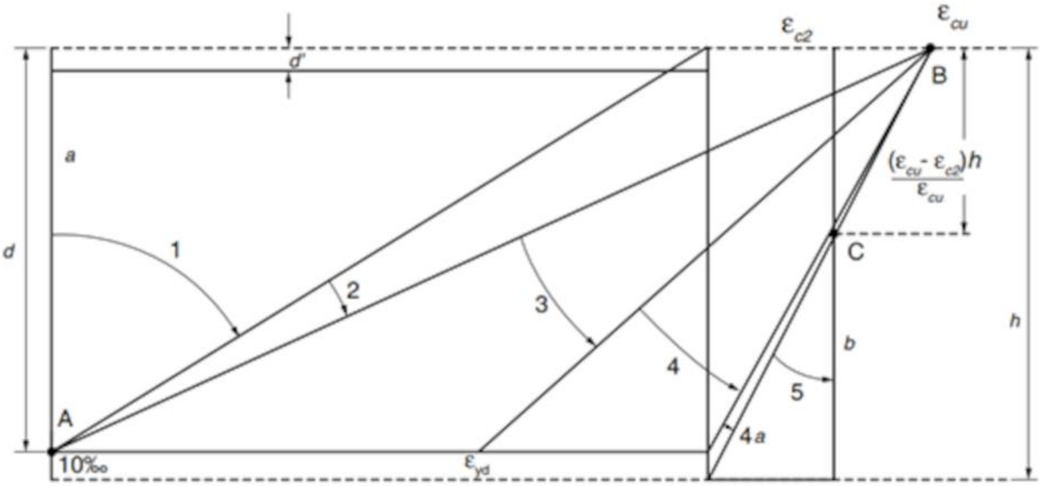

Figure 1. Domains and limit state of a transversal cross-section. Source: ABNT (2014).

Given the multiple physical and geometric parameters that must be analyzed in combination in order to reach an optimized design of the column cross-section, computational techniques were developed to study the influence of the variation of these parameters and how they can be combined in favor of a more refined result.

Optimization algorithms can take a deterministic or heuristic approach. Deterministic methods generally consider a derivable objective function and, regardless of how many times it is executed, the same result is obtained for the same defined starting point. Heuristic methods, usually called probabilistic methods, consider random values each time the code is executed, resulting in different results data in each execution.

The main advantages of heuristic methods when compared to deterministic ones are: not requiring the objective function to be derivable and the possibility of using both continuous and discrete parameters or even a combination of both. The biggest drawback is the processing time.

The Genetic Algorithm (GA) is a faster heuristic optimization method than others of the same type. They are based on the theory of natural selection and evolution of species, in which the fittest individuals, that is, the individuals that have a better value in the function objective, survive.

The literature shows the frequent use of the genetic algorithm, and that it can be applied to slabs (Alabbasi, Hussein, Abdeljaber, & Avci, 2020; Malveiro, Ribeiro, Sousa, & Calçada, 2018; Theyssen et al., 2021); beams (Abdel Nour, Vié, Chateauneuf, Amziane, & Kallassy, 2021; Pérez, Cladera, Rabuñal, & Abella, 2010; Shahnewaz, Machial, Alam, & Rteil, 2016; Solhmirzaei, Salehi, Kodur, & Naser, 2020); frame (Di Trapani, Malavisi, Marano, Sberna, & Greco, 2020; Gaetani d'Aragona, Polese, & Prota, 2020); columns (Li, Zhang, Shi, Wu, & Li, 2021); bridge elements (Chisari, Bedon, & Amadio, 2015; Kamjoo & Eamon, 2018; Martí, Gonzalez-Vidosa, Yepes, & Alcalá, 2013; Pachón, Castro, García-Macías, Compan, & Puertas, 2018; Ribeiro, Calçada, Delgado, Brehm, & Zabel, 2012); wind power towels (de Lana et al., 2021); reservoir (Stanton & Javadi, 2014); concrete railway barriers (Yin, Fang, Wang, & Wen, 2016); semi-rigid expansion joints made of steel and composite (Ramires, Andrade, Vellasco, & Lima, 2012); reinforced concrete beam-column joints (Sengupta & Li, 2013); smooth steel bars (Di Sarno, Pugliese, & De Risi, 2021); and the final cost of a reinforced concrete building (Sahab, Ashour, & Toropov, 2005).

Given the exposed idea, the objective of this work was to identify, for a 10-floor building, the optimal dimensions of a rectangular reinforced concrete column, as well as an optimized reinforcement arrangement, resulting in a lower cost that meets all the requirements of the NBR 6118 (ABNT, 2014), through the development of a computational code with a genetic algorithm approach.

Material and methods

Case study - Calculation of characteristic forces and eccentricity

It is considered a 2 m high corner column, that supports beams with 20 x 40 cm cross-section, which, in turn, supports a 10 cm high slab with dimensions of 5 x 6 m, as it can be seen in Figure 2. This column is on the ground floor of a building with 10 floors. To consider the characteristic load per floor, the weight strength of the reinforced concrete pieces (Equation 1) and the occupation load (Equation 2) are calculated using the information given by the NBR 6120 (ABNT, 2019), as can be seen in Equation 3:

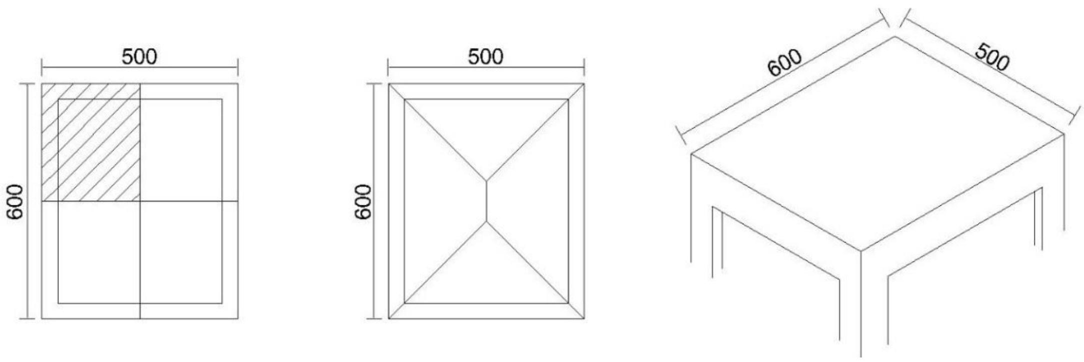

Figure 2. Dimensions of the case study problem.

$$\gamma_{conc} = \frac{25kN}{m^3} \quad (1)$$

$$Q = 1{,}5\ kN/m^2 \quad (2)$$

$$N_k = P_{slab} + P_{beam} + Q$$
$$= 25 \times [(2.5 \times 3.0 \times 0.1) + (2.5 \times 0.10 \times 0.40) + (3 \times 0.10 \times 0.40)] + 1{,}5 \times (2.5 \times 3.0) \quad (3)$$
$$N_k = 40{,}78\ kN$$

In which γ_{conc} is the concrete's specific weight, Q is the beam's load of occupation, N_k is the characteristic normal force, P_{slab} is the weight of the slab, and P_{beam} is the weight of the beams.

The loads on the beam in the x-direction are calculated by Equation 4 and the maximum moment by Equation 5, and equally in the y-direction by Equation 6 and Equation 7:

$$q_x = G_{slab} + Q_{slab} + G_{beam} = \frac{(\gamma_{conc} \times V_{slab}) + (Q \times A_{slab}) + (\gamma_{conc} \times V_{beam})}{l}$$
$$= \left\{(25 \times 0.1 + 1.5) \times \left[\left(\frac{5 \times 2.5}{2}\right)/5\right]\right\} + (25 \times 0.10 \times 0.40) = 6\ kN/m \quad (4)$$

$$M_x = \frac{ql^2}{12} = \frac{6 \times 5^2}{12} = 12.5\ kN \cdot m \quad (5)$$

$$q_y = G_{slab} + Q_{slab} + G_{beam} = \frac{(\gamma_{conc} \times V_{slab}) + (Q \times A_{slab}) + (\gamma_{conc} \times V_{beam})}{l}$$
$$\left\{(25 \times 0.1 + 1.5) \times \left[\left(\frac{(6+1) \times 3}{2}\right)/6\right]\right\} + (25 \times 0.10 \times 0.40) = 9\frac{kN}{m} \quad (6)$$

$$M_y = \frac{ql^2}{12} = \frac{9 \times 6^2}{12} = 27\ kN \cdot m \quad (7)$$

In which q_x and q_y are the loads distributed on the beams, G_{slab} is the slab load on the beams, Q_{slab} is the occupation load of the slabs on the beams, G_{beam} is the load of the weight of the beams, V_{slab} is the contribution volume of the slab, A_{slab} is the contribution area of the slab, V_{beam} is the beam volume, l is the beam length, and M_x and M_y are the bending moments that are transferred to the columns.

The floors are considered equal, so the bending moment at the top and at the base of the columns are equal, and in the center is null. As the column cross-section is unknown so far, the following calculations are assumed for the purpose of requested forces, considering the dimensions of the column proportional to the requesting moments. Equation 8 presents the estimate of the column area, and Equation 9, Equation 10, and Equation 11 present the previous calculation of dimensions.

$$A_0 = \frac{N_{s,d}}{0.5 \times f_{ck}} = \frac{1.4 \times (10 \times 40.78kN)}{0.5 \times \frac{3.5kN}{cm^2}} = 326.24\ cm^2 \geq 360\ cm^2 \quad (8)$$

$$\frac{h_x}{M_{s,x}} \sim \frac{h_y}{M_{s,y}} \quad (9)$$

$$h_x \times h_y = A_0 \quad (10)$$

$$\left(\frac{M_{s,x}}{M_{s,y}} h_y\right) \times h_y = A_0 \quad .\because \quad h_y = 27.89 \quad .\because \quad h_x = 12.91 \quad (11)$$

In which A_0 is the column cross-section area, $N_{s,d}$ is the design normal force, f_{ck} is the characteristic compressive strength of concrete, h_x is the horizontal dimension of the cross-section, and h_y is the vertical dimension of the cross-section.

Considering the minimum dimension as 20 cm according to the NBR 6118 (ABNT, 2014), without taking into account the increase in load, the initial dimensions of the cross-section for calculation of forces are 20 x 28 cm.

The calculations of the eccentricities are as follows:

a) Geometric information: effective length (Equation 12), bending moments in the columns (Equation 13), and slenderness coefficient (Equation 14):

$$l_e \geq \{\ l\ ,\ \ l_0 + h_{x,y}\ \} \tag{12}$$

In which l_e is the effective length, l is the axis-to-axis length equal to the floor height, l_0 the value inside the beams equal to the value of the ceiling height, and $h_{x,y}$ the dimensions of the columns in both directions. So, if $h_x = 20\ cm$, and $h_y = 28\ cm$, leads to $l_{ex} = 240\ cm$ and

$l_{ey} = 240\ cm.$

$$M_{top} = M_{bottom} = M_{eng}\,\frac{\frac{3I_{column}}{l_{column}}}{\frac{4I_{beam}}{l_{beam}} + \frac{6I_{column}}{l_{column}}} \tag{13}$$

where M_{top} and M_{bottom} are the bending moments absorbed by the top and the bottom of the column, M_{eng} is the bending moment previously calculated, I_{column} and I_{beam} are the mass moment of inertia of the column and the beam, l_{column}, and l_{beam} are the lengths of the column and the beam. So, $M_{top,bottom\,x} = 2.21\ kN \cdot m$ and $M_{top,bottom\,y} = 7.60\ kN \cdot m$.

$$\lambda_x = \frac{l_{ex}\sqrt{12}}{h_x} = 41.57\ \ ;\ \ \lambda_y = \frac{l_{ey}\sqrt{12}}{h_y} = 29.70 \tag{14}$$

In which λ is the slenderness coefficient, l_e is the effective length and h is the cross-section's height in the analyzed direction.

b) First-order eccentricity

The initial eccentricity values can be seen in Equation 15 with the already represented variables.

$$e_{ix} = \frac{M_{engx}}{N_d} = 0.387\ cm\ \ ;\ \ e_{ix} = \frac{M_{engx}}{N_d} = 1.33\ cm \tag{15}$$

The θ parameter can be calculated by Equation 16 for the accidental eccentricity calculation by Equation 17.

$$\frac{1}{400} \leq \theta_1 = \frac{1}{100\sqrt{l_{ef}}} \leq \frac{1}{200}\ \ .\because\ \ \theta_{1x} = \theta_{1y} = \frac{1}{154.9}\ \ .\because\ \ \theta_{1x} = \theta_{1y} = \frac{1}{200} \tag{16}$$

$$e_{ax} = e_{ay} = \theta_1\,\frac{l}{2} = 0.6\ cm \tag{17}$$

The minimum eccentricity to be considered by the NBR 6118 (ABNT, 2014) can be calculated by Equation 18.

$$e_{min} = 1.5 + 0{,}03.h\ \ .\because\ \ e_{min,x} = 2.1\ cm\ \ ;\ \ e_{min,y} = 2.34\ cm \tag{18}$$

The first-order eccentricity is the largest value between the minimum eccentricity and the sum of the initial and accidental eccentricity, as seen in Equation 19.

$$e_1 = e_i + e_a \geq e_{min}\ \ .\because\ \ e_{1x} = 2.1\ cm\ \ ;\ \ e_{1y} = 2.34\ cm \tag{19}$$

c) Slenderness verification

For the slenderness coefficient in each interval below, it is necessary to make certain considerations to increase the eccentricities. For $\lambda \leq \lambda_1$, it is considered a low slenderness or robust column, considering only the first-order eccentricity. For $\lambda_1 < \lambda \leq 90$, there is an average slenderness column, which requires a consideration of second-order effects. For $90 < \lambda \leq 140$, there is a high slenderness column, and for $140 < \lambda \leq 200$ there is an exceedingly slenderness column, which requires the consideration of the column creeping. Reinforced concrete columns with $\lambda \geq 200$ are not dimensioned. The λ_1 parameter depends on the value of α_b (Equation 20) and can be calculated by Equation 21.

$$0.4 \leq \alpha_b = 0.6 + 0.4 \times \frac{M_{top}}{M_{bottom}} \leq 1\ \ .\because\ \ \alpha_{b,x} = \alpha_{b,y} = 1 \tag{20}$$

$$\lambda_1 = \frac{25+12.5\times\frac{e_1}{h}}{\alpha_b} \leq 35 \ \therefore \ \lambda_{1,x} = 26.31 \ ; \ \lambda_{1,y} = 26.04 \qquad (21)$$

In which λ_1 is the limit slenderness, e_1 is the initial eccentricity, h is the height of the cross-section in the analyzed direction, and α_b is calculated based on the bending moments in the top and the base of the column.

Therefore, it is necessary to carry out second-order considerations for both eccentricities.

d) Second-order eccentricity depends on the column curvature and dimensionless normal forces, as presented in Equation 22.

$$e_2 = \frac{l_e^2}{10}.\frac{1}{r} \ ; \ \frac{1}{r} = \frac{0.005}{h(\nu+0.5)} \leq \frac{0.005}{h} \ ; \ \nu = \frac{N_{sd}}{A_c \times f_{cd}}$$

$$\nu = \frac{1.4\times(10\times40.78)}{(20\times28)\times3.5} = 0.2913 \ ; \ \left(\frac{1}{r}\right)_x = 0.00025 \ ; \ \left(\frac{1}{r}\right)_y = 0.000179 \qquad (22)$$

$$e_{2,x} = 2.88\ cm \ ; \ e_{2,y} = 2.06\ cm$$

In which e_2 is the second-order eccentricity, l_e is the effective length, $\frac{1}{r}$ is the column curvature, h is the height of the cross-section in the analyzed direction, ν is the dimensionless normal force, N_{sd} is the design normal force, A_c is the concrete cross-section area, f_{cd} is the design concrete strength (defined by $f_{ck}/1.4$).

e) Total eccentricities in the x and y direction can be calculated by Equation 23 and Equation 24 as the sum of the first and second-order eccentricities.

$$e_{tot,x} = e_{1,x} + e_{2,x} = 4.98\ cm \qquad (23)$$

$$e_{tot,y} = e_{1,y} + e_{2,y} = 4.40\ cm \qquad (24)$$

Therefore, the main data for requesting forces are the characteristic normal force of 40.78 kN, eccentricity in x and y direction respectively of 4.98 cm and 4.40 cm.

Algorithm for columns verification

By using the Scilab programming language, it was possible to develop an engineering software based on the definition of the ultimate limit state domains of NBR 6118 (ABNT, 2014), in order to calculate the resistance forces of a rectangular and symmetrical reinforced concrete column. The method is based on receiving the geometry (height, base, steel layers in x and y directions, diameters of transverse and longitudinal steel rebar) and material properties (f_{ck} and f_{yk}) of the column, which generate an envelope graph of applied design normal forces versus resistant moments for x and y directions. The method is obtained by varying the neutral line from zero to a value higher than the studied cross-section. The issue of the actual bending effort being oblique and not normal was simplified by the reduction of the resistance efforts in both directions, therefore receiving a reduction due to the smallest neutral line found, that is, the most critical case between the two directions (Araújo, 2014). The requesting design parameters, characteristic normal strength and eccentricities are compared to the envelope strengths and other normative parameters to see if the cross-section has design errors.

Initially, the necessary constants for the calculations used were defined. All constants were taken from design parameters or the materials availability from the responsible engineer. They are: requesting force in kN; eccentricities in both directions in cm; a concrete layer of coverage in cm according to the NBR 6118 (ABNT, 2014); maximum aggregate diameter in cm; characteristic strength at 28 days of concrete age in $kN \cdot cm^{-2}$; characteristic strength of steel to yield in $kN \cdot cm^{-2}$; modulus of elasticity of reinforced concrete in $kN \cdot cm^{-2}$; number of floors; cost of concrete per cubic meter and steel cost per kilogram, in terms of the currency (the Brazilian currency was used, as known as real); steel density in kg m^{-3}; slab and column heights in cm.

In this work, the values of geometric dimensions were generated randomly. The variables that receive these values are column cross-section height in cm, column cross-section base in cm, vertical steel layers, horizontal steel layers, the diameter of transverse steel in cm (commercial values), and diameter of longitudinal steel in cm (commercial values).

Initially, the normal force design was calculated. The NBR 6118 (ABNT, 2014) defines a multiplicative factor of 1.4 for the force multiplied by a load factor if any of the dimensions (d) is less than 19 cm, as defined by $\gamma_n = 1.95 - 0.05 \times d$. Finally, the characteristic forces from each floor are multiplied by the number of floors.

The verification of the area also comes from the NBR 6118 (ABNT, 2014), which says that the minimum area section of the column must be 360 cm^2. The diameter of the longitudinal rebar check says that it must be greater than 5 mm and a quarter of the diameter of the longitudinal rebar. The diameter of the longitudinal rebar check says that it must be greater than 10 mm and less than an eighth of the smallest dimension of the column cross-section. The minimum longitudinal reinforcement rate in terms of area of steel is 0.4% of the concrete cross-section area or $0.15 \times N_s/f_{yk}$, and the minimum rate is 8% of the concrete cross-section. The maximum number of longitudinal layers is given by the dimension of the cross-section minus the concrete covers, the diameters of the transverse rebar, and the longitudinal rebar diameter (distance to the axis) divided by the minimum spacing, which is defined by the longitudinal rebar diameter plus the largest value between 1.2 times the aggregate diameter, the longitudinal rebar diameter itself and 2 cm.

Based on the dimensions of the cross-section, the need for supplementary stirrups is calculated if the region that is between the outermost longitudinal rebar axis and 20 times the diameter of the transverse rebar does not include any rebar. Thus, a supplementary stirrup must be used in this location.

The constants defined for the envelope calculations are: the bending moments defined by the design normal force multiplied by the eccentricities; concrete stress defined by 1.4 design normal divided by 0.85 area; and the distance to the centroid of the most tensioned rebar, defined by the coverage added to the transverse gauge and half of the longitudinal gauge.

To perform the envelope calculation, first, the steel area of each layer of the cross-section is calculated by varying the variable "i", from 1 to the number of layers, with the number of rebars in the first and last layer being equal to the number of layers in the other direction. To define the resistant forces, the neutral line is varied from 0 to the limit of 4/3 of the cross-section size in the considered direction with 0.01 intervals. Assuming the limit value times 100, that is, if the height is 30 cm, the neutral line assumes 4,000 progressive values. The factor "g" then varies from 1 to 100 times the described limit, parallel to the variation of the neutral line value. The neutral line defines, based on the domains observed in Figure 1, the values of the concrete and steel reactions, which also define the resistant normal force and the resistant bending moments for each normal force. Considering the domain limits, the reactions are defined as it follows (the variable d being the distance from the most compressed face to the most tensioned rebar):

- For the neutral line greater than 1.25 times the analyzed dimension: the force of the concrete is 0.85 of the area times the design compressive strength. Force is applied at the center of the cross-section.

- For the neutral line below the limit previously described and greater than 3.5×d/13.5: the concrete force is 0.8 of the area (neutral line value times the dimension in the other direction) times the design compressive strength. Force is applied at 0.4 of the neutral line.

- For the neutral line below the limits described above: the concrete force is 0.8 of the area (neutral line value times the dimension in the other direction) times the design compressive strength weighted by the neutral line factor divided by 3.5×d /13.5. Force is applied at 0.4 of the neutral line.

- For the neutral line less than 3.5×d/13.5: the steel traction force in each layer below the neutral line is proportional to the distance between the most tensioned rebar (with a maximum design yield stress) to the neutral line. The force is applied at the proportional centroid of the forces (constant stress at 1% deformation).

- For the neutral line above the limit described previously and below 3.5×d/5.5704: the steel traction force in each layer under the neutral line is proportional to the distance between the most tensioned rebar (with maximum yield stress of design) to the neutral line. The force is applied at the proportional centroid of the forces (deformation ranging from 1% to 0.30704%).

- For the neutral line above the limits described previously and below the size of "d": the steel traction force in each layer under the neutral line is proportional to the distance between the most tensioned rebar and the neutral line. The force is applied at the proportional centroid of the forces (steel tension varies from maximum yield with 0.30704% deformation linearly to zero tension at 0% deformation).

- For the neutral line above "d", the steel reaction is zero.

The normal resistance as a function of the neutral line is given by the sum of forces, in this case, concrete reaction force minus steel reaction forces. The resistant bending moment as a function of the neutral line is given by the reaction of the concrete and steel multiplied by the respective application distances, added to the normal resistant reaction multiplied by the neutral line value. Therefore, the normal resistance is reduced as a function of the proportion of the neutral line value divided by the dimension "d" for each neutral line value, in order to obtain the graph reduced in both directions. However, the reduction is not performed only if the neutral line is greater than the analyzed section size.

A graph of the normal force lessened by the resistant bending moments is plotted. For the lessened normal resisting force that is equal to the design requesting force, the resistive bending moment in that direction is adopted, which is also compared to the requesting moments, as defined by the requesting design normal force times the eccentricities. If the moment does not suffice this verification, an error is indicated in the steel of the analyzed direction.

To calculate the column value, the concrete column volume is calculated and multiplied by the previously defined concrete value. The value of steel is simply defined by the sum of weights from the longitudinal rebar, transverse rebar, and stirrups multiplied by the value of the steel as a function of the weight. In the end, it sums up to obtain the final value of the column.

Genetic algorithm

The Genetic Algorithm (GA), created by John Holland in the 1960s, consists of an optimization algorithm inspired by Charles Darwin's theory, which defends the idea that only individuals with more advantageous characteristics could survive and reproduce (Coley, 1999). The structure of the AG is shown in Figure 3.

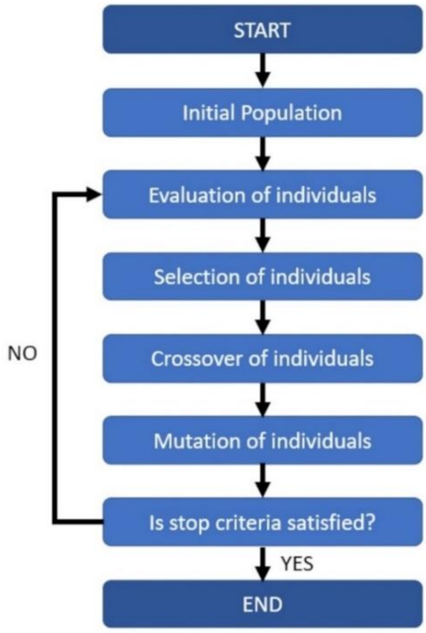

Figure 3. Genetic Algorithm Structure.

For the genetic algorithm, a population of 280 individuals was established. These individuals have as variable characteristics: the height of the cross-section (H), the base of the cross-section (B), the number of layers in the direction of the Y-axis (cy), the number of layers in the direction of the X-axis (cx), the transverse reinforcement steel bar (bittrans) and the longitudinal reinforcement rebar (bitlong). In this work, each individual fills a column of information in the matrix of population versus characteristics. Variables were randomly defined for each individual by a tool that randomizes a factor between 0 and 1 and multiplies values that were initially determined as maximum value. For example, if it was previously defined that the maximum height of the cross-section was 100 cm, the algorithm would randomize any value between 0 and 100 cm. In the case of the reinforcement steel bar diameter, which has defined values, it was randomized and rounded to the closest diameter. Once defined those variables, all individuals were evaluated and verified according to the NBR 6118 (ABNT, 2014), as previously explained.

The objective function of this algorithm and the main characteristic that will define what is the most optimized cross-section for the column is the cost of the column, which considers the amount of concrete and steel used. For the cost evaluation of all individuals of the population, they were penalized with an increase in the value of individuals who do not meet the normative verifications. The more unverified characteristics, the bigger the penalization, which will increase its final cost.

The selection operator compares individuals randomly and selects those with the lowest penalized costs to reproduction, thus generating new individuals in a new population. The crossover operator used was the Simulated Binary Crossover (SBX), which, from the two selected individuals, generates two new individuals with similar characteristics (Deb & Agrawal, 1995). As in genetics, a mutation may occur in which the heirs do not resemble their parents, so, for the mutation operator, a rate of 5% of mutation was adopted by using a randomized variable. When this random tool returns a number between 0 and 0.05, only the variable is randomized again, just like in the first calculation of the population. The stopping criteria was defined by the number of generations equal to 100.

The code was executed thirty times to verify that the result obtained was in fact the global best, and not just a local best.

Results and discussion

After processing the genetic algorithm, the characteristics of the column with the lowest cost are shown in Table 1. The optimized cross-section for this column would have this characteristic because it was the minimum cost achieved through the algorithm, making it the most economical solution based on the part of the algorithm that makes the verification.

Table 1. Characteristics of the column with the lowest cost.

H	B	cy	cx	Bittrans	Bitlong	Cost
31.60 cm	31.65 cm	2	3	0.5 cm	1.0 cm	R$ 138.55

For the analysis of how the genetic algorithm works, it was chosen five graphical representations of all the individuals that had passed through evaluation in the algorithm.

The first graph (Figure 4) shows cross-section areas of all individuals that passed through the algorithm versus their penalized costs, demonstrating how the algorithm uses the fitness function to separate individuals based on the number of errors detected. The noticeable lines are the amount of errors considered, and they show how the penalty separates the verified columns, in blue, from the unverified ones, in red. It was demonstrated that the verified individuals maintain a lower cost because they were not penalized, which allow them to be more likely to produce heirs.

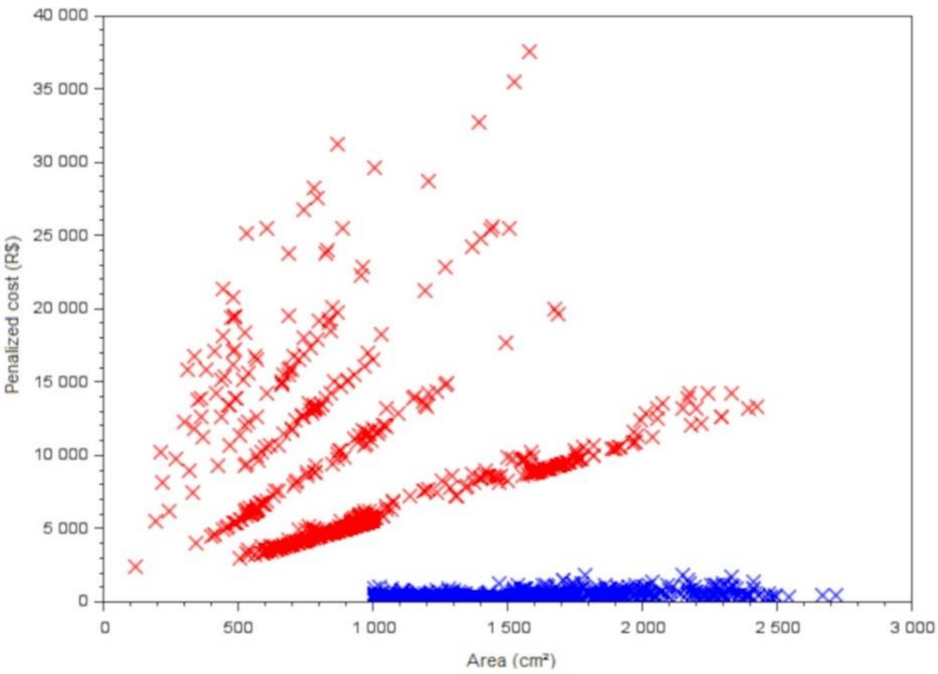

Figure 4. Area (cm^2) vs Penalized cost of the total individuals (R$).

The second graph (Figure 5) plots cross-section areas of all the verified individuals that passed through the algorithm versus its cost and shows that the dispersion of the best-selected individuals creates a density in smaller values that may or may not be related to smaller areas, which reinforces the proposition that the cheapest columns will have more generations associated with them.

The third graph (Figure 6) shows cross-section areas of all individuals that passed through the algorithm versus their costs without penalization, evidencing that if there were no fitness function, several individuals with an error would be vying for the lowest value. It also shows that, despite the errors, these individuals could generate others who approached the optimal values without errors (near the blue cloud).

The fourth graph (Figure 7) plots the generations when a cheaper verified individual appears, evidencing that not all generations of the code were able to generate better individuals than the previous generations, which justifies the use of 100 generations to find an ideal individual. The more generations, the more possible it is to find the most optimized individual based on its cost.

Finally, the last graph (Figure 8) brings the average cost of all individuals through the generations and shows that over the generations, the average penalized cost of the entire population approaches the optimal value, thus generating a population with more individuals without errors and penalties. Once again, this shows the functioning of a genetic algorithm based on the best individuals within a population.

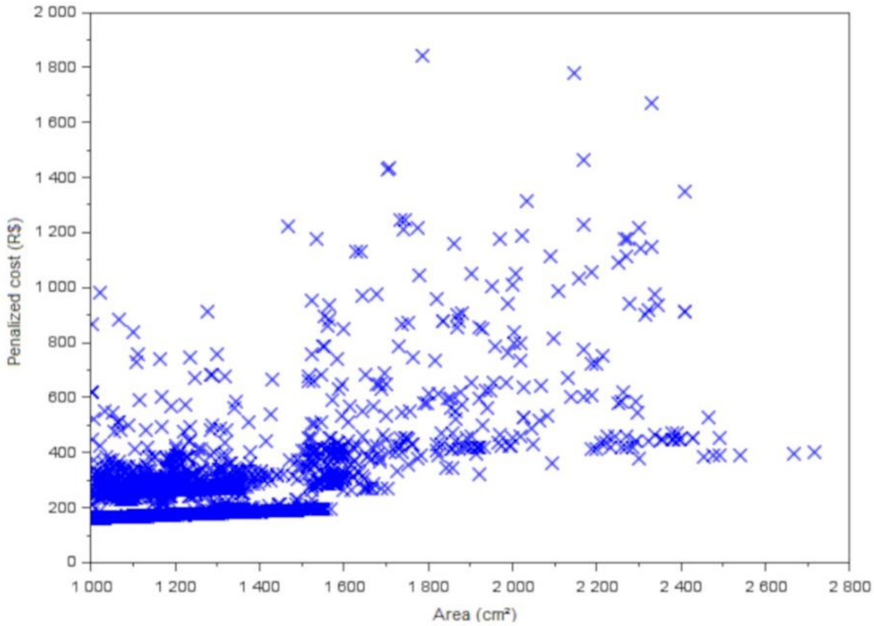

Figure 5. Area (cm²) vs Penalized cost of the non-errors' individuals (R$).

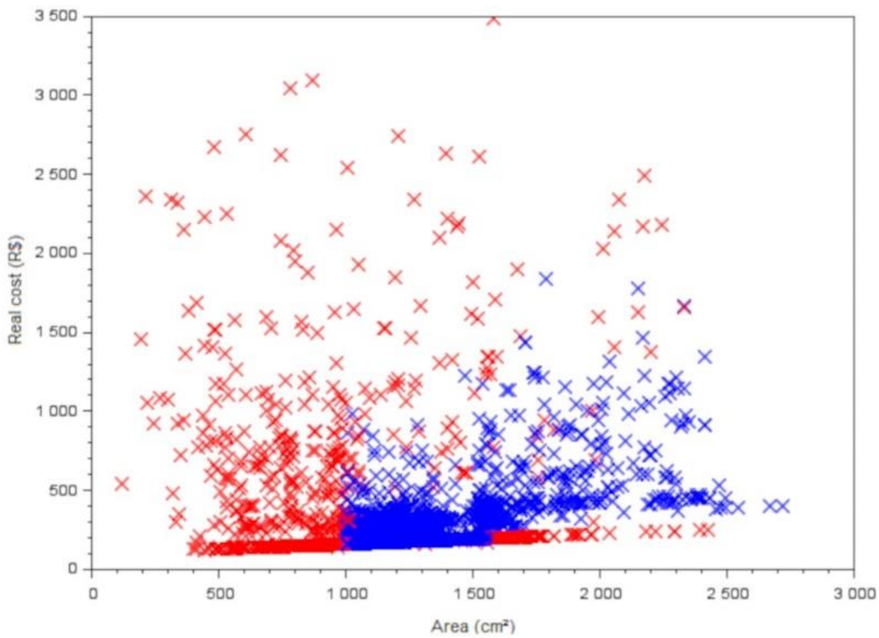

Figure 6. Area (cm²) vs Real cost of the total individuals (R$).

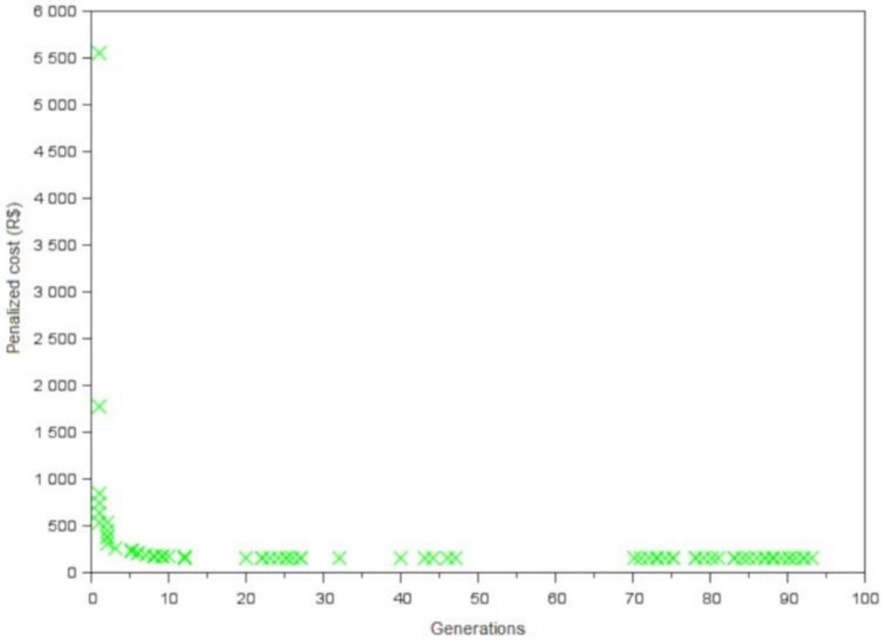

Figure 7. Generations vs Penalized cost of the lower-cost individual (R$).

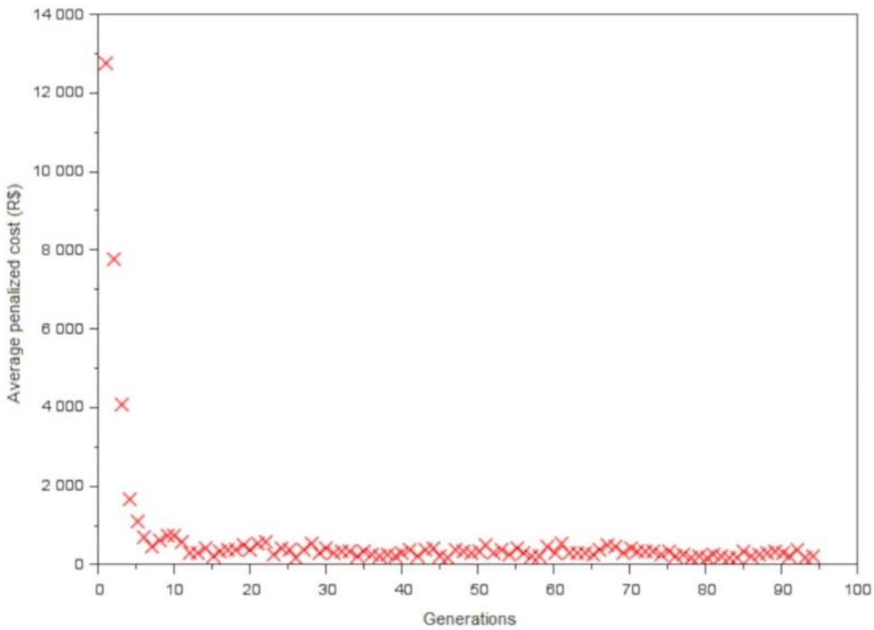

Figure 8. Generation vs Average of penalized costs (R$).

Conclusion

It was possible to perform a column verification code with oblique requests. The developed algorithm can be used for field engineering checks and it can also be adapted for optimizing beams or slabs. In addition, it was possible to implement the GA with cost evaluation. Furthermore, it was concluded that genetic algorithms are good sources of different parameters that make up the cross-sections of reinforced concrete pieces. The different algorithms with different numbers of populations and generations proposed during the production of this work showed that larger populations increase the chance of getting the global minimum in cost, that is, the most optimized column.

Acknowledgements

We would like to thank the Coordination of Superior Level Staff Improvement (CAPES) - Brazil for the financial support of one of the authors.

References

Abdel Nour, N., Vié, D., Chateauneuf, A., Amziane, S., & Kallassy, A. (2021). Design of partially prestressed concrete beams, optimization of T-shaped section with heels. *Engineering Structures*, *235*, 112054. DOI: https://doi.org/10.1016/j.engstruct.2021.112054

Alabbasi, S., Hussein, M., Abdeljaber, O., & Avci, O. (2020). A numerical and experimental investigation of a special type of floating-slab tracks. *Engineering Structures*, *215*, 110734. DOI: https://doi.org/10.1016/j.engstruct.2020.110734

Araújo, J. M. (2014). *Curso de concreto armado* (Vol. 1, 4. ed.). Rio Grande, RS: Dunas.

Associação Brasileira de Normas Técnicas [ABNT]. (2014). *Projeto de estruturas de concreto – Procedimento. (NBR, 6118)*. Rio de Janeiro, RJ: ABNT.

Associação Brasileira de Normas Técnicas [ABNT]. (2019). *Ações para o cálculo de estruturas de edificações. (NBR, 6120).* Rio de Janeiro, RJ: ABNT.

Carvalho, R. C., & Pinheiro, L. M. (2013). *Cálculo e detalhamento de estruturas usuais de concreto armado* (Vol. 2). São Paulo, SP: PINI.

Chisari, C., Bedon, C., & Amadio, C. (2015). Dynamic and static identification of base-isolated bridges using Genetic Algorithms. *Engineering Structures*, *102*, 80-92. DOI: https://doi.org/10.1016/j.engstruct.2015.07.043

Coley, D. A. (1999). *An introduction to genetic algorithms for scientists and engineers*. World Scientific Publishing Company.

de Lana, J. A., Júnior, P. A. A. M., Magalhães, C. A., Magalhães, A. L. M. A., Andrade Junior, A. C., & Ribeiro, M. S. B. (2021). Behavior study of prestressed concrete wind-turbine tower in circular cross-section. *Engineering Structures*, *227*, 111403. DOI: https://doi.org/10.1016/j.engstruct.2020.111403

Deb, K., & Agrawal, R. B. (1995). Simulated binary crossover for continuous search space. *Complex Systems*, *9*, 115-148.

Di Sarno, L., Pugliese, F., & De Risi, R. (2021). Non-linear finite element optimization for inelastic buckling modelling of smooth rebars. *Engineering Structures*, *240*(4), 112378. DOI: https://doi.org/10.1016/j.engstruct.2021.112378

Di Trapani, F., Malavisi, M., Marano, G. C., Sberna, A. P., & Greco, R. (2020). Optimal seismic retrofitting of reinforced concrete buildings by steel-jacketing using a genetic algorithm-based framework. *Engineering Structures*, *219*, 1-14. DOI: https://doi.org/10.1016/j.engstruct.2020.110864

Gaetani d'Aragona, M., Polese, M., & Prota, A. (2020). Stick-IT: A simplified model for rapid estimation of IDR and PFA for existing low-rise symmetric infilled RC building typologies. *Engineering Structures*, *223*, 111182. DOI: https://doi.org/10.1016/j.engstruct.2020.111182

Kamjoo, V., & Eamon, C. D. (2018). Reliability-based design optimization of a vehicular live load model. *Engineering Structures*, *168*, 799-808. DOI: https://doi.org/10.1016/j.engstruct.2018.05.033

Li, Z. X., Zhang, X., Shi, Y., Wu, C., & Li, J. (2021). Predication of the residual axial load capacity of CFRP-strengthened RC column subjected to blast loading using artificial neural network. *Engineering Structures*, *242,* 1-15. DOI: https://doi.org/10.1016/j.engstruct.2021.112519

Malveiro, J., Ribeiro, D., Sousa, C., & Calçada, R. (2018). Model updating of a dynamic model of a composite steel-concrete railway viaduct based on experimental tests. *Engineering Structures*, *164*, 40-52. DOI: https://doi.org/10.1016/j.engstruct.2018.02.057

Martí, J. V., Gonzalez-Vidosa, F., Yepes, V., & Alcalá, J. (2013). Design of prestressed concrete precast road bridges with hybrid simulated annealing. *Engineering Structures*, *48*, 342-352. DOI: https://doi.org/10.1016/j.engstruct.2012.09.014

Pachón, P., Castro, R., García-Macías, E., Compan, V., & Puertas, E. (2018). E. Torroja's bridge: Tailored experimental setup for SHM of a historical bridge with a reduced number of sensors. *Engineering Structures*, *162*, 11-21. DOI: https://doi.org/10.1016/j.engstruct.2018.02.035

Pérez, J. L., Cladera, A., Rabuñal, J. R., & Abella, F. M. (2010). Optimal adjustment of EC-2 shear formulation for concrete elements without web reinforcement using Genetic Programming. *Engineering Structures*, *32*(11), 3452-3466. DOI: https://doi.org/10.1016/j.engstruct.2010.07.006.

Ramires, F. B., Andrade, S. A. L., Vellasco, P. C. G. S., & Lima, L. R. O. (2012). Genetic algorithm optimization of composite and steel endplate semi-rigid joints. *Engineering Structures*, *45*, 177-191. DOI: https://doi.org/10.1016/j.engstruct.2012.05.051

Ribeiro, D., Calçada, R., Delgado, R., Brehm, M., & Zabel, V. (2012). Finite element model updating of a bowstring-arch railway bridge based on experimental modal parameters. *Engineering Structures*, *40*, 413-435. DOI: https://doi.org/10.1016/j.engstruct.2012.03.013

Sahab, M. G., Ashour, A. F., & Toropov, V. V. (2005). Cost optimisation of reinforced concrete flat slab buildings. *Engineering Structures*, *27*(3), 313-322. DOI: https://doi.org/10.1016/j.engstruct.2004.10.002

Sengupta, P., & Li, B. (2013). Modified Bouc-Wen model for hysteresis behavior of RC beam-column joints with limited transverse reinforcement. *Engineering Structures*, *46*, 392-406. DOI: https://doi.org/10.1016/j.engstruct.2012.08.003

Shahnewaz, M., Machial, R., Alam, M. S., & Rteil, A. (2016). Optimized shear design equation for slender concrete beams reinforced with FRP bars and stirrups using Genetic Algorithm and reliability analysis. *Engineering Structures*, *107*, 151-165. DOI: https://doi.org/10.1016/j.engstruct.2015.10.049

Solhmirzaei, R., Salehi, H., Kodur, V., & Naser, M. Z. (2020). Machine learning framework for predicting failure mode and shear capacity of ultra high performance concrete beams. *Engineering Structures*, *224*, 111221. DOI: https://doi.org/10.1016/j.engstruct.2020.111221

Stanton, A., & Javadi, A. A. (2014). An automated approach for an optimised least cost solution of reinforced concrete reservoirs using site parameters. *Engineering Structures*, *60*, 32-40. DOI: https://doi.org/10.1016/j.engstruct.2013.12.020

Theyssen, J. S., Aggestam, E., Zhu, S., Nielsen, J. C. O., Pieringer, A., Kropp, W., & Zhai, W. (2021). Calibration and validation of the dynamic response of two slab track models using data from a full-scale test rig. *Engineering Structures*, *234*, 1-17. DOI: https://doi.org/10.1016/j.engstruct.2021.111980

Yin, H., Fang, H., Wang, Q., & Wen, G. (2016). Design optimization of a MASH TL-3 concrete barrier using RBF-based metamodels and nonlinear finite element simulations. *Engineering Structures*, *114*, 122-134. DOI: https://doi.org/10.1016/j.engstruct.2016.02.009